Glycobiology vol. 19 no. 9 pp. 950–957, 2009
doi:10.1093/glycob/cwp089
Advance Access publication on June 19, 2009

COMMUNICATION

The specific localization of seminolipid molecular species on mouse testis during testicular maturation revealed by imaging mass spectrometry

Naoko Goto-Inoue[1,2], Takahiro Hayasaka[2], Nobuhiro Zaima[2], and Mitsutoshi Setou[2]

[2]Department of Molecular Anatomy, Hamamatsu University School of Medicine, 1-20-1 Handayama, Higashi-ku, Hamamatsu, Shizuoka 431-3192, Japan

Received on April 20, 2009; revised on June 14, 2009; accepted on June 15, 2009

More than 90% of the glycolipid in mammalian testis consists of a unique sulfated glyceroglycolipid called seminolipid. The galactosylation of the molecule is catalyzed by UDP-galactose:ceramide galactosyltransferase (CGT). Disruption of the CGT gene in mice results in male infertility due to the arrest of spermatogenesis, indicating that seminolipid plays an important role in reproductive function. Seminolipid molecules can be assigned to different molecular species based on the fatty acid composition. In this report, we investigated the localizations of the molecular species of seminolipid by imaging mass spectrometry and demonstrated that major molecule (C16:0-alkyl-C16:0-acyl) was expressed throughout the tubules: some (C16:0-alkyl-C14:0-acyl and C14:0-alkyl-C16:0-acyl) were predominantly expressed in spermatocytes and the other (C17:0-alkyl-C16:0-acyl) was specifically expressed in spermatids and spermatozoa. This is the first report to show the cell-specific localization of each molecular species of seminolipid during testicular maturation.

Keywords: imaging/MALDI/mass spectrometry/seminolipid/testis

Introduction

Two major sulfoglycolipids are produced by mammals: sulfatide, which is a sphingolipid, and seminolipid, which is an ether glycerolipid (Ishizuka 1997). The galactosylation of these sulfoglycolipids is catalyzed by a common enzyme, UDP-galactose:ceramide galactosyltransferase (CGT, EC 2.4.1.45) (Honke et al. 1996, 2002). CGT-deficient mice, which completely lack the ability to produce sulfatide and seminolipid, are generated (Coetzee et al. 1996). CGT-deficient mice manifest certain neurological disorders due to myelin dysfunction and an arrest of spermatogenesis, indicating that the sulfoglycolipids are essential for both myelin formation and spermatogenesis. Seminolipid is synthesized in primary spermatocytes and remains stable during spermatogenesis. It is essential for mammalian development that this process occurs normally (Fujimoto et al. 2000), although the precise role of seminolipid in spermatogenesis and other processes that take place during and following egg fertilization is still not completely understood. Glycolipids self-associate in cellular membranes to form a microdomain referred to as a lipid raft (Simons and Ikonen 1997). It is suggested that seminolipid is present in the lipid raft (Rodemer et al. 2003) and contributes to the sperm cell membrane shape and stability (Attar et al. 2000; Bou Khalil et al. 2006) since it is also involved in recognition events (at least 20 proteins with affinity to seminolipid have been identified) and cell–cell adhesion. Specifically, seminolipid on the mammalian sperm head surface has direct affinity for the egg zona pellucida (ZP) and is an integral component of sperm lipid rafts, which are the ZP binding microdomains (White et al. 2000; Weerachatyanukul et al. 2001; Bou Khalil et al. 2006). In order to develop a better understanding of the molecular mechanisms associated with sulfoglycolipids, a powerful tool is needed to follow the localization of each sulfoglycolipid in tissue. Seminolipid was identified as a single molecular structure with the general composition: 1-*O*-alkyl-2-*O*-acyl-3-*O*-D-(3-sulfo)-galactopyranosyl-*sn*-glycerol. While most naturally occurring glycolipids exhibit a high degree of heterogeneity in their alkyl and acyl chain lengths, seminolipids from boar (Ishizuka et al. 1973), rat (Kornblatt et al. 1972), human (Ueno et al. 1977), and bovine (Alvarez et al. 1990) spermatozoa are composed mainly of hexadecyl and hexadecanoyl chains (M.W. 796), respectively. In the past decades, several antibodies against sulfoglycolipids have been produced and are currently in widespread use (Ishizuka 1997). Sulph-1, which has high specificity to sulfoglycolipids, has been widely used for immunostaining of seminolipid to identify its tissue localization (Zhang et al. 2005). However, because each of these antibodies recognizes all sulfoglycolipids, including sulfatide, lactosylsulfatide, and seminolipid, none of them is effective for detecting these molecules individually. In addition, it is impossible to identify individual molecular species having different fatty acid chains. In CGT-deficient mice, which lack seminolipid, testicular germ cells after meiosis are absent, whereas spermatogonia and early spermatocytes appear normal (Tadano-Aritomi and Ishizuka 2003). The results of studies in CGT-deficient mice support the general idea that cell surface seminolipid molecules are functionally important in germ cell differentiation and/or interactions with other cell types (Hakomori 2000). However, the specific molecular species of seminolipid involved in these events remain unknown. It is quite important to determine what kind of seminolipid exists on each cell in order to clarify the molecular assembly formed in the glycolipid microdomain.

[1]To whom correspondence should be addressed: Tel: +81-53-435-2085; Fax: +81-53-435-2292; e-mail: naoko.goto.inoue@gmail.com

In this report, we used imaging mass spectrometry (IMS) to investigate the localization of different molecular species of seminolipid, which are classified based on their fatty acid composition. IMS has several advantages for exploring the two-dimensional distribution of lipids: first, IMS does not require any labels or specific probes to investigate the localization; second, IMS is a nontargeted imaging method, allowing us to detect the localization of unexpected metabolites; finally, IMS allows the simultaneous imaging of many types of molecular species of lipid. IMS has been widely applied to the analysis of tissues sections, and predominantly detects lipids, which are the most abundant molecules in tissue (Shimma et al. 2007, 2008; Hayasaka et al. 2008; Sugiura et al. 2008). Accordingly, the technique of IMS is widely applied in the field of lipid research. Seminolipid is the major glycolipid in testes, so in negative ion mode analyses, seminolipid is likely to be the predominantly detected molecule, allowing us to readily identify its localization.

Results and discussion

Seminolipid composition of testis

The sulfated glycerogalactolipid seminolipid is the main glycolipid in mammalian spermatozoa and testis (Ishizuka et al. 1973; Ishizuka 1997). In the present study, thin-layer chromatography (TLC) revealed a fine single band of seminolipid in total lipid extracts of mouse testes (Figure 1A). In the samples from 2-week-old mouse testes, the band of seminolipid was weaker than in the samples from 8-week-old mice. The reason for this finding was that seminolipid is mainly found in spermatocytes, spermatids, and spermatozoa, but 2-week-old testes do not contain spermatids and spermatozoa. There are some molecular species of seminolipid which have a variety of alkyl and acyl chains. In this report, we tried to identify the composition of seminolipid molecular species of mouse testes by the method of TLC-Blot-MALDI IMS. This method, which can detect and visualize molecular species of lipids on the PVDF membrane, has already been reported by the authors (Goto-Inoue et al. 2008). To determine what molecular species exist, we tried to achieve a single MS spectrum to the transferred band of seminolipid on the PVDF membrane. As we conducted MS analysis of the seminolipid band, we observed a simple spectrum in which the $[M-H]^-$ ions (*m/z* 767, 795, 809, 821, and 823) were detected (Figure 1B). Then, we performed IMS of *m/z* 767, 795, 809, 821, and 823 as target molecules of seminolipid on the PVDF membrane. Figure 1C shows the imaging results of *m/z* 767, 795, 809, 821, and 823, respectively. These results indicated that these peaks were predominantly detected in the band on the PVDF membrane, suggesting that these peaks were the seminolipid molecular species.

Structural analyses of seminolipid molecules

We performed subsequent MS/MS analyses to obtain fragment ions which are able to identify alkyl and acyl chains. Previous reports have shown that the elimination of the acyl residue (a) was predominant (Tadano-Aritomi et al. 2003), furthermore other fragment ions derived from elimination of fatty acid, (b), (c), and (d), would be observed in MS/MS analyses of seminolipid molecules (Alvarez et al. 1990) (Figure 2A). Indeed, in the MS/MS spectrum produced by collision-induced dissociation (CID) of $[M-H]^-$ (*m/z* 795) ion, the fragment ion at *m/z* 539 (a) was most abundant, as described previously (Tadano-Aritomi et al. 2003), and (b), (c), and (d) ions (*m/z* 255, 299, and 241) (Attar et al. 2000) were detected, respectively (Figure 2B). According to the same scheme of fragmentation, in the MS/MS spectrum produced by CID of $[M-H]^-$ (*m/z* 767) ion, the fragment ion at *m/z* 539 (a) was detected which was derived from the elimination of 228 (C14:0), and (b), (c), and (d) ions (*m/z* 227, 299, and 241, respectively) were also detected (Figure 2C). The result revealed that *m/z* 767 was the seminolipid (C16:0-alkyl-C14:0-acyl). Furthermore, we also detected *m/z* 511 (a′) ion which was derived from the elimination of 256 (C16:0). The fragment (b′) and (c′) ions (*m/z* 255 and 299) were also detected. These results indicated that *m/z* 767 included another structure (C14:0-alkyl-C16:0-acyl) when the alkyl and acyl chains were replaced. In the MS/MS spectrum of the precursor ion at $[M-H]^-$ (*m/z* 809), the fragment ion at *m/z* 553 (a) was the most abundant peak and was derived from the elimination of 256 (C16:0) (Figure 2D). Other fragment ions (b), (c), and (d) (*m/z* 255, 299, and 255, respectively) were also observed. The result demonstrated that *m/z* 809 was the seminolipid (C17:0-alkyl-C16:0-acyl). In the MS/MS spectra of precursor ions at *m/z* 821 and 823, the fragment ions at *m/z* 565 (a) and 567 (a) were observed predominantly. These fragment ions were derived from the elimination of 256 (C16:0). In addition, although their peak intensities were low, the fragment (b), (c), and (d) ions (*m/z* 255, 299, and 267, respectively) derived from *m/z* 821, and (*m/z* 255 and 299) derived from *m/z* 823, were also detected in the MS/MS spectra. The amount of (d) ion in the MS/MS spectrum of *m/z* 823 as a precursor was too small to be observed. These results demonstrated that *m/z* 821 and 823 were the seminolipid molecules (C18:1-alkyl or C18:0-alkenyl-C16:0-acyl) and (C18:0-alkyl-C16:0-acyl), respectively (Figure 2E and F). In addition, we found the weak common fragment ions at *m/z* 539 (a′), *m/z* 299 (c′), and *m/z* 241 (d′) in the MS/MS spectra of precursor ions at *m/z* 821 and 823. The fragment (a′) ions were derived from the elimination of 282 (C18:1) and 284 (C18:0), and (d′) ions were derived from the elimination

Table I. Seminolipid molecular species and their relative intensity in the TLC-Blot-MALDI MS spectrum and imaging mass spectrum

Molecular species	*m/z*	Relative intensity (%) on the PVDF membrane	Relative intensity (%) on the tissue section	
			2 weeks	8 weeks
C16:0-alkyl-C14:0-acyl C14:0-alkyl-C16:0-acyl	767	6.5	1.2	6.1
C16:0-alkyl-C16:0-acyl	795	85.4	96.6	77.6
C17:0-alkyl-C16:0-acyl	809	3	0.6	11.4
C18:1-alkyl or C18:0-alkenyl-C16:0-acyl C16:0-alkyl-C18:1-acyl	821	2.3	0.8	2.8
C18:0-alkyl-C16:0-acyl C16:0-alkyl-C18:0-acyl	823	1.8	0.8	2.1

The *sn*-1 position contains an ether-linked alkyl group and the *sn*-2 position contains an acyl chain. The relative intensity (%) represents the relative ratio of a specific ion peak to the sum intensity of the total five peaks detected.

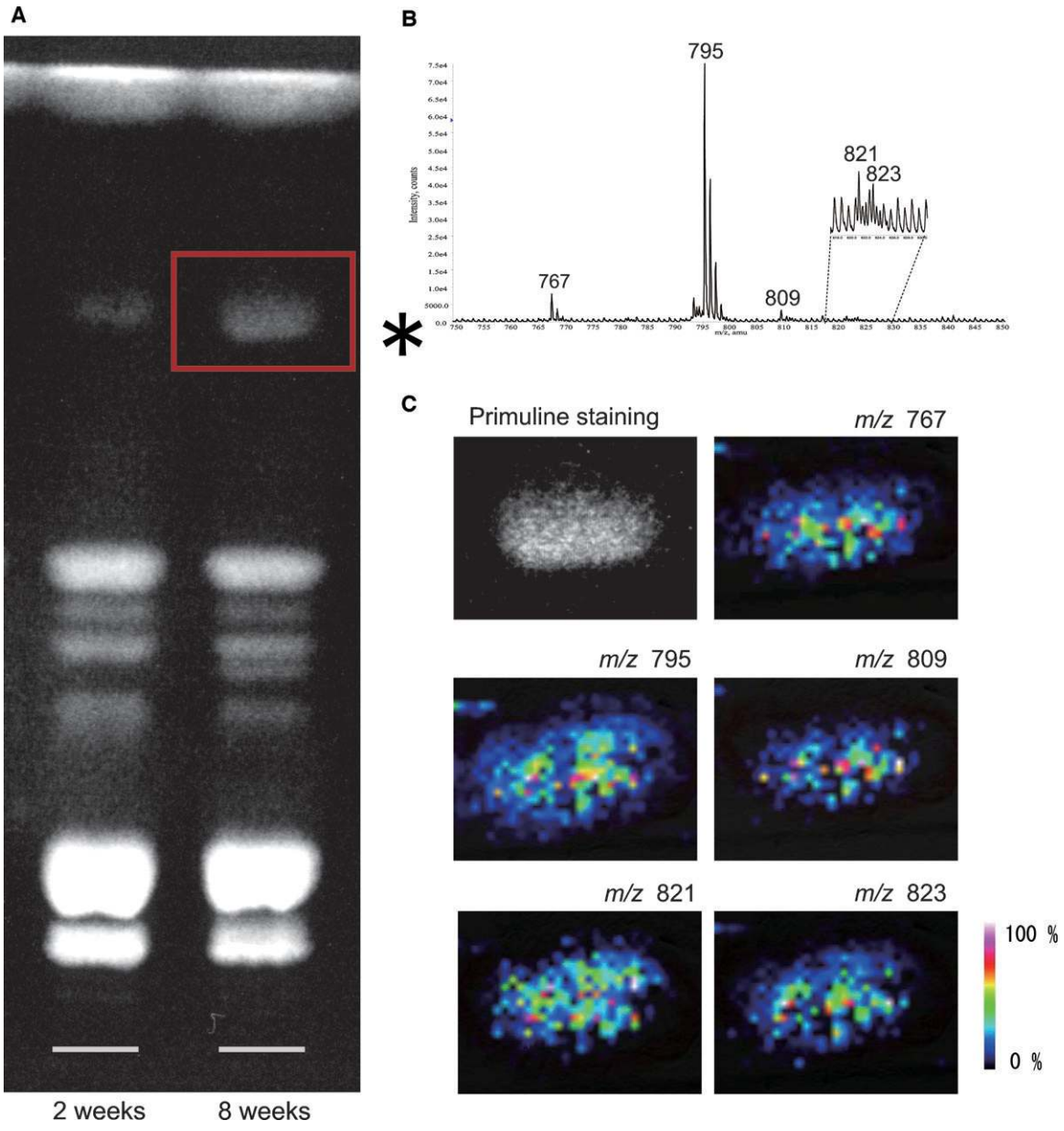

Fig. 1. TLC analysis and TLC-Blot-MALDI IMS analyses of lipids extracted from mouse testes. TLC analysis of lipids extracted from 2-week-old (left) and 8-week-old (right) mouse testes (**A**), and TLC-Blot-MALDI MS spectrum (**B**) and ion images of TLC-Blot-MALDI IMS obtained from the band of seminolipid molecules on the PVDF membrane (**C**) are shown.

of C16:0-alkyl chains. The results suggested that *m/z* 821 and 823 included another structure (C16:0-alkyl-C18:1-acyl) and (C16:0-alkyl-C18:0-acyl), respectively. Thus, MS/MS analyses of each of the peaks detected by TLC-Blot-MALDI IMS clearly revealed that all detected peaks on the PVDF membrane were molecular species of seminolipid, and clarified their alkyl and acyl chains (Table I). The molecular species at *m/z* 767, 821, and 823 have two possible structures resulting from the replacement of their alkyl and acyl chains. Because the intensity of (a) ions was higher than that of (a′) ions, which were derived from the elimination of the acyl chain, we considered that *m/z* 767 (C16:0-alkyl-C14:0-acyl), *m/z* 821(C18:1-alkyl or C18:0-alkenyl-C16:0-acyl), and *m/z* 823(C18:0-alkyl-C16:0-acyl) were major components.

Detection of seminolipid molecules directly on mouse testes by imaging mass spectrometry

We performed IMS analyses of the testes at 2 and 8 weeks of age to investigate the localization of seminolipid molecular species. In mice at the age of 2 weeks, spermatogenesis was still progressing, and the cell stage of spermatocyte was late pachytene. Mice at the age of 8 weeks had already completed the spermatogenesis process, and all cell types were observed (Tadano-Aritomi et al. 2003). In the MS spectrum obtained from the testis of 2-week-old mice, *m/z* 795 was detected predominantly, *m/z* 767 was detected though the intensity was low, and other molecules were barely detected. An IMS spectrum obtained from the testis of 8-week-old mice was almost the same as that of TLC-blot-MALDI IMS of the seminolipid

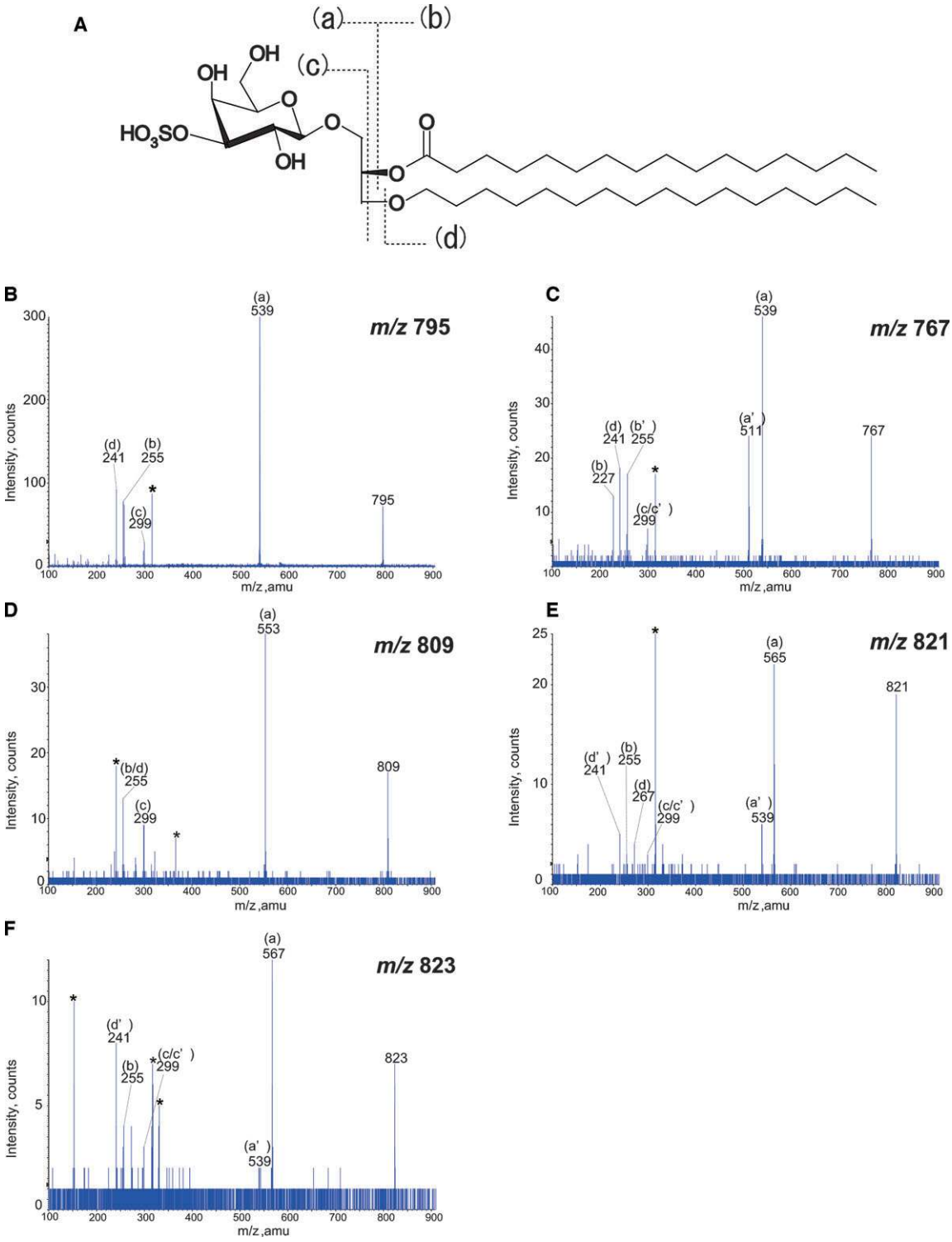

Fig. 2. Fragmentation scheme and MS/MS spectra of seminolipid molecules. The nomenclatures for cleavages of precursor ions of seminolipid molecules (**A**) and MS/MS spectra obtained with the precursor ions at *m/z* 795 (**B**), 767 (**C**), 809 (**D**), 821 (**E**), and 823 (**F**) are shown. Asterisks show unidentified ions.

extracted from 8-week-old mice (Table I and Figure 3A). There were no substantial differences in the relative intensity between the TLC-blot-MALDI MS spectrum and IMS spectrum on 8-week-old mice tissues except for *m/z* 809. It is suggested that ion suppression of minor molecules occurred on concentrated bands on the PVDF membrane (Table I). Moreover, the results of MS/MS analyses of detected peaks on tissues (data not shown) were identical with the results on the PVDF membrane showed in Figure 2. These results have demonstrated that detected peaks on testes were derived from seminolipid molecules. Figure 3B

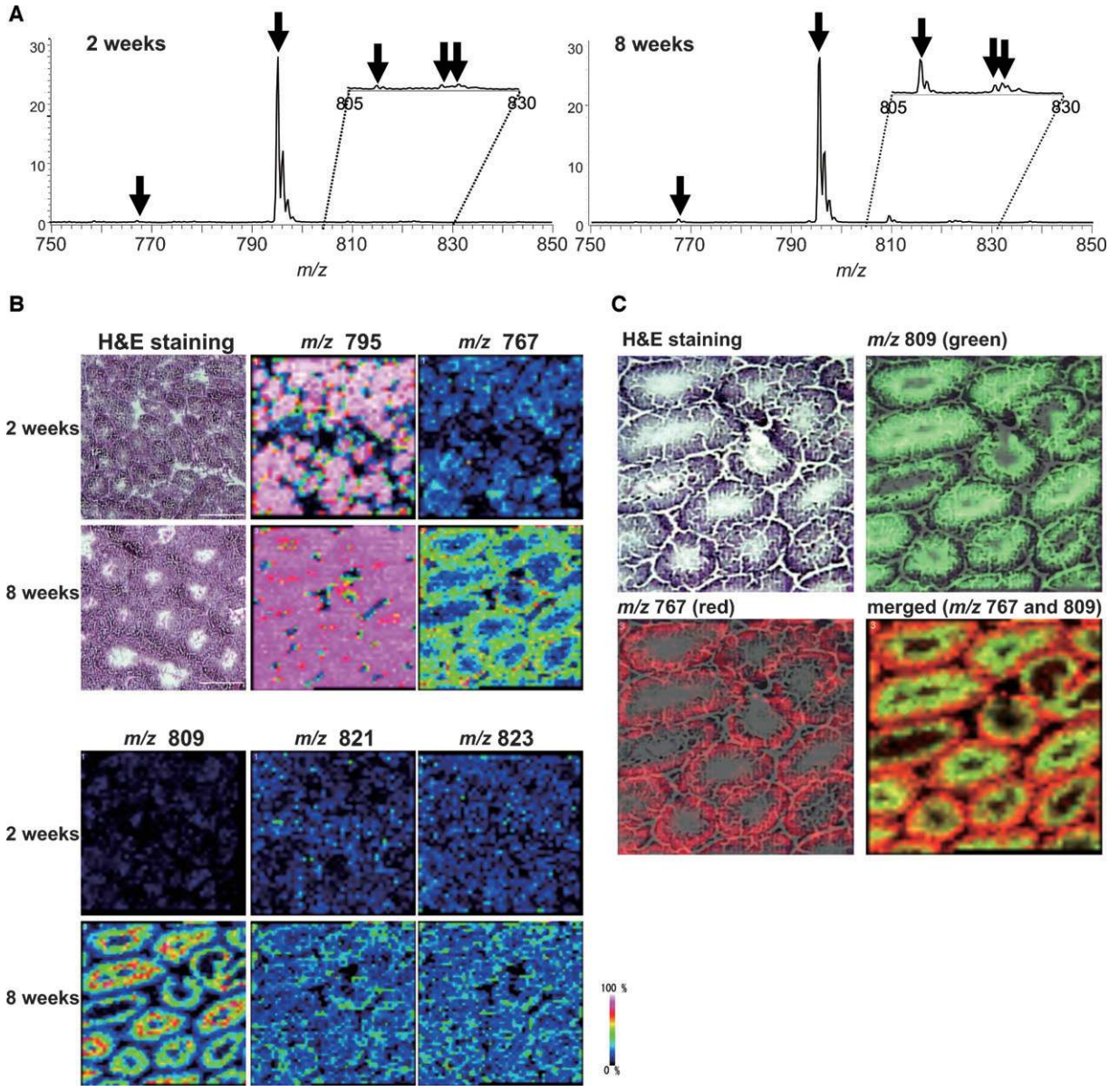

Fig. 3. MS spectrum obtained from mouse testes and ion images of seminolipid molecules on mouse testes. (**A**) The overall spectra of 2- and 8-week-old testes are shown. (**B**) The optical image of the sample stained with H&E staining, and ion images obtained from 2- and 8-week-old mouse testes are shown. (**C**) The optical image of H&E staining of the same cryo-section which was stained after IMS is shown. The ion images at *m/z* 767 and 809 obtained from 8-week-old mouse testes are merged with the image of H&E staining. The merged ion image of *m/z* 767 and 809 is also shown. Bar: 400 μm.

shows ion images of the testes at 2 and 8 weeks of age. We observed a major seminolipid, *m/z* 795 (C16:0-alkyl-C16:0-acyl), throughout the tubules in both 2- and 8- week-old samples. This result corresponded with previously reported results of the immunostaining of Sulph-1 (Zhang et al. 2005). Next, we investigated the localization of a minor seminolipid, *m/z* 767 (C16:0-alkyl-C14:0-acyl or C14:0-alkyl-C16:0-acyl). We found that *m/z* 767 localized at the edge of tubules, where spermatogonia and spermatocytes exist. Some previous reports have shown that seminolipid was expressed on the plasma membranes of spermatogonia, spermatocytes, spermatids, and spermatozoa, as evidenced by the immunostaining of testes, but another report showed that seminolipid was synthesized in primary spermatocytes and appeared as early as day 8 of age (Fujimoto et al. 2000, 2001). The present findings demonstrated that *m/z* 767 is strongly expressed on spermatocytes. The molecules at *m/z* 821 and *m/z* 823 were existed throughout the tubules though their peak intensities were low, and the intensities were weaker for the samples from 2-week-old mice than in those from 8-week-old mice. It seems that various seminolipid molecular species are appearing according to testicular maturation. To identify the detailed localization of molecules which showed cell-specific expression, we tried to overlay these ion images to the optical image of the same cryo-section which was stained after IMS. We showed that these molecules clearly existed in tubules, and the merged image of *m/z* 767 and 809 demonstrated that these molecules had different distributions (Figure 3C). It has been reported that spermatocytes are important for spermatogenesis

because the coordination of germ cell differentiation might be mediated by surface interactions between spermatocytes and Sertoli cells (Tadano-Aritomi and Ishizuka 2003). The molecule at *m/z* 767, which is a spermatocyte-specific seminolipid molecule, is suggested to be important for spermatogenesis (Fujimoto et al. 2000; Honke et al. 2002). On the other hand, *m/z* 809 was expressed in contrast to *m/z* 767. The molecule was expressed in the inner lumen of tubules of 8-week-old testes and was not clearly detected in 2-week-old testes (Table I). In the vicinity of the lumen, spermatids and spermatozoa exist only at 8-week-old testes. So our results indicated that *m/z* 809 was a spermatid- and spermatozoon-specific seminolipid. It has been suggested that seminolipid is involved in the interaction between sperm and egg because seminolipid is present in the sperm head microdomain (Moase et al. 1997). As a spermatid- and spermatozoon-specific seminolipid, *m/z* 809 might be involved in the sperm–egg interaction.

In this report, we demonstrated that each molecular species of seminolipid showed a different pattern of expression during testicular maturation. These results suggested that these molecular species serve different cellular functions. For example, the odd number fatty acid, which was catalyzed by α-oxidation, is minor component in mammalian tissue. It has been reported that α-oxidation is catalyzed by phytanoyl-CoA 2-hydroxylase and 2-hydroxyphytanoyl-CoA lyase (Foulon et al. 2005; Wierzbicki 2007). Because the molecule at *m/z* 809 (C17:0-alkyl-C16:0-acyl), which has the odd number fatty acid and is catalyzed by these enzymes, is specifically expressed in spermatids and spermatozoa, we expect that these enzymes act specifically in these cells. Several reports have suggested that odd-numbered fatty acids and very-long-chain polyunsaturated fatty acids, which are unusual molecules in mammals, are characteristic fatty acids in testes (Poulos et al. 1986; Robinson et al. 1992; Aveldano et al. 1993). In another study, the authors showed that both simple glycans and the particular acyl chains of germinal sphingolipids are relevant for proper completion of meiosis (Rabionet et al. 2008). And, in the previous study, phytanoyl-CoA hydroxylase knockout mice (a mouse model for Refsum disease) on a phytol diet did not have the full complement of spermatogenic cells. This showed that α-oxidation in testes is essential for male reproductive function (Ferdinandusse et al. 2008). So, our hypothesis is that a sperm-specific seminolipid which has odd-numbered fatty acid might also contribute to male reproductive function.

Because of the lack of the specific antibody, the distributional analysis of lipids is one of the obsolete fields. The ability of IMS to determine the distinct localization of each molecular species is quite valuable. Because of this characteristic of IMS, the technique could be used to perform distributional analyses of various lipids in tissue. Seminolipid-associated molecules should be identified as a first step in determining the function of seminolipid molecules. The present results should be helpful for determining which molecular species contribute to reproductive function.

Material and methods

Chemicals

All solvents used for MS were of HPLC grade and were purchased from Kanto Chemical Co., Inc. (Tokyo, Japan). Bradykinin and angiotensin-II were obtained from Sigma-Aldrich Japan (Tokyo, Japan) and used as calibration standards. 2,5-Dihydroxy benzoic acid (DHB) obtained from Bruker Daltonics (Leipzig, Germany) was used as the matrix. We used the testes of C57BL/6Cr mice from Japan SLC (Shizuoka, Japan) at the indicated time points (2 and 8 postnatal weeks). The mice were sacrificed and tissues were used for the analyses by TLC and imaging mass spectrometry.

Thin-layer chromatography

Testes samples (11 mg) from 2-week-old and 8-week-old C57BL/6Cr mice were homogenized with chloroform/methanol (1:2), and lipids were extracted by the method of Bligh and Dyer (1959). Each extracted sample was applied as 5 mm spots to silica gel 60 HPTLC plates (Merck, Darmstadt, Germany). Plates were developed with a solvent system of methylacetate/propanol/chloroform/methanol/0.25% aqueous $CaCl_2$ (25/25/25/10/9, v/v/v/v). After developing of samples, the HPTLC plate was sprayed with 0.1% primuline reagent until it became wet, and then was air-dried thoroughly. Lipid bands were visualized under UV light at 365 nm.

TLC-Blot-MALDI MS and MS/MS analysis

The methods used for the TLC-Blot-MALDI MS and MS/MS analyses were described previously (Goto-Inoue et al. 2008). These analyses were performed using a MALDI-hybrid quadrupole TOF-type mass spectrometer (QSTAR XL; Applied Biosystems/MDS Sciex, Foster City, Canada) equipped with an orthogonal MALDI source. Samples were analyzed in negative ionization mode over the range of *m/z* 100–2000. The MS spectra were calibrated externally using a standard peptide calibration mixture containing 10 pmol/μL each of bradykinin peptide fragment (amino acid residue 1–7) ($[M-H]^-$, *m/z* 755.40) and human angiotensin-II peptide fragment ($[M-H]^-$, *m/z* 1044.54). In MS/MS analyses, the selectivity of the precursor ion was increased by selecting high mass selection mode. The collision energy was changed according to the precursor ion to achieve good mass spectra.

Tissue preparation

The extirpated tissue blocks of testes were immediately frozen in aliquot nitrogen. The frozen sections were sliced with a cryostat (Leica CM 1950; Leica, Wetzlar, Germany) at a thickness of 8 μm. Frozen sections were thaw-mounted on indium-tin-oxide (ITO)-coated glass slides (Bruker Daltonics). We used a DHB solution (50 mg/mL; 70% methanol) as the matrix. The matrix solution was uniformly sprayed over the tissue surface using a 0.2 mm nozzle caliber air-brush (Procon Boy FWA Platinum; Mr. Hobby, Tokyo, Japan). Frozen sections were also thaw-mounted on MAS-coated glass slides (Matsunami Glass Industries, Ltd, Osaka, Japan) for conventional hematoxilin-eosin (H&E) staining.

Imaging mass spectrometry

IMS were performed using a MALDI time-of-flight (TOF)/TOF-type instrument (Ultraflex 2 TOF/TOF; Bruker Daltonics). This instrument was equipped with a 355 nm Nd:YAG laser. The data were acquired in the negative reflectron mode by using an external calibration method. In this analysis, signals over the range of *m/z* 400–2000 were collected. The raster scan

on the tissue surface or PVDF membrane was performed automatically by FlexControl and Fleximaging 2.0 software (Bruker Daltonics). The number of laser irradiations was 200 shots in each spot. Image reconstruction was performed using FlexImaging 2.0 software. These samples were analyzed at the same time, and the total ion current of each raster point was normalized for semi-quantitative analyses (Sugiura et al. 2008; Yao et al. 2008; Ageta et al. 2009).

Funding

The SENTAN program of the Japan Science and Technology Agency to M.S and Young scientists B (21780110) to N. G-I.

Conflict of interest statement

None declared.

Abbreviations

CID, collision-induced dissociation; CGT, UDP-galactose: ceramide galactosyltransferase; IMS, imaging mass spectrometry; TLC, thin layer chromatography; ZP, zona pellucida.

References

Ageta H, Asai S, Sugiura Y, Goto-Inoue N, Zaima N, Setou M. 2009. Layer-specific sulfatide localization in rat hippocampus middle molecular layer is revealed by nanoparticle-assisted laser desorption/ionization imaging mass spectrometry. *Med Mol Morphol.* 42(1):16–23.

Alvarez JG, Storey BT, Hemling ML, Grob RL. 1990. High-resolution proton nuclear magnetic resonance characterization of seminolipid from bovine spermatozoa. *J Lipid Res.* 31(6):1073–1081.

Attar M, Kates M, Bou Khalil M, Carrier D, Wong PT, Tanphaichitr N. 2000. A Fourier-transform infrared study of the interaction between germ-cell specific sulfogalactosylglycerolipid and dimyristoylglycerophosphocholine. *Chem Phys Lipids.* 106(2):101–114.

Aveldano MI, Robinson BS, Johnson DW, Poulos A. 1993. Long and very long chain polyunsaturated fatty acids of the n-6 series in rat seminiferous tubules. Active desaturation of 24;4n-6 to 24;5n-6 and concomitant formation of odd and even chain tetraenoic and pentaenoic fatty acids up to C32. *J Biol Chem.* 268(16):11663–11669.

Bligh EG, Dyer WJ. 1959. A rapid method of total lipid extraction and purification. *Can J Biochem Physiol.* 37(8):911–917.

Bou Khalil M, Chakrabandhu K, Xu H, Weerachatyanukul W, Buhr M, Berger T, Carmona E, Vuong N, Kumarathasan P, Wong PT, et al. 2006. Sperm capacitation induces an increase in lipid rafts having zona pellucida binding ability and containing sulfogalactosylglycerolipid. *Dev Biol.* 290(1):220–235.

Coetzee T, Fujita N, Dupree J, Shi R, Blight A, Suzuki K, Suzuki K, Popko B. 1996. Myelination in the absence of galactocerebroside and sulfatide: Normal structure with abnormal function and regional instability. *Cell.* 86(2):209–219.

Ferdinandusse S, Zomer AW, Komen JC, Van Den Brink CE, Thanos M, Hamers FP, Wanders RJ, Van Der Saag PT, Poll-The BT, Brites P. 2008. Ataxia with loss of Purkinje cells in a mouse model for Refsum disease. *Proc Natl Acad Sci USA.* 105(46):17712–17717.

Foulon V, Sniekers M, Huysmans E, Asselberghs S, Mahieu V, Mannaerts GP, Van Veldhoven PP, Casteels M. 2005. Breakdown of 2-hydroxylated straight chain fatty acids via peroxisomal 2-hydroxyphytanoyl-CoA lyase: A revised pathway for the alpha-oxidation of straight chain fatty acids. *J Biol Chem.* 280(11):9802–9812.

Fujimoto H, Tadano-Aritomi K, Ishizuka I, Suzuki K. 2001. Functional analysis of glycolipids in galactosylceramide synthase (CGT)-deficient mice: Arrest of male meiosis and compensation of renal function. *Tanpakushitsu Kakusan Koso.* 46(1):45–53.

Fujimoto H, Tadano-Aritomi K, Tokumasu A, Ito K, Hikita T, Suzuki K, Ishizuka I. 2000. Requirement of seminolipid in spermatogenesis revealed by UDP-galactose:ceramide galactosyltransferase-deficient mice. *J Biol Chem.* 275(30):22623–22626.

Goto-Inoue N, Hayasaka T, Sugiura Y, Taki T, Li YT, Matsumoto M, Setou M. 2008. High-sensitivity analysis of glycosphingolipids by matrix-assisted laser desorption/ionization quadrupole ion trap time-of-flight imaging mass spectrometry on transfer membranes. *J Chromatogr B Anal Technol Biomed Life Sci.* 870(1):74–83.

Hakomori SI. 2000. Cell adhesion/recognition and signal transduction through glycosphingolipid microdomain. *Glycoconj J.* 17(3–4):143–151.

Hayasaka T, Goto-Inoue N, Sugiura Y, Zaima N, Nakanishi H, Ohishi K, Nakanishi S, Naito T, Taguchi R, Setou M. 2008. Matrix-assisted laser desorption/ionization quadrupole ion trap time-of-flight (MALDI-QIT-TOF)-based imaging mass spectrometry reveals a layered distribution of phospholipid molecular species in the mouse retina. *Rapid Commun Mass Spectrom.* 22(21):3415–3426.

Honke K, Hirahara Y, Dupree J, Suzuki K, Popko B, Fukushima K, Fukushima J, Nagasawa T, Yoshida N, Wada Y, et al. 2002. Paranodal junction formation and spermatogenesis require sulfoglycolipids. *Proc Natl Acad Sci USA.* 99(7):4227–4232.

Honke K, Yamane M, Ishii A, Kobayashi T, Makita A. 1996. Purification and characterization of 3′-phosphoadenosine-5′-phosphosulfate:GalCer sulfotransferase from human renal cancer cells. *J Biochem.* 119(3):421–427.

Ishizuka I. 1997. Chemistry and functional distribution of sulfoglycolipids. *Prog Lipid Res.* 36(4):245–319.

Ishizuka I, Suzuki M, Yamakawa T. 1973. Isolation and characterization of a novel sulfoglycolipid, "seminolipid," from boar testis and spermatozoa. *J Biochem.* 73(1):77–87.

Kornblatt MJ, Schachter H, Murray RK. 1972. Partial characterization of a novel glycerogalactolipid from rat testis. *Biochem Biophys Res Commun.* 48(6):1489–1494.

Moase CE, Kamolvarin N, Kan FW, Tanphaichitr N. 1997. Localization and role of sulfoglycolipid immobilizing protein 1 on the mouse sperm head. *Mol Reprod Dev.* 48(4):518–528.

Poulos A, Sharp P, Johnson D, White I, Fellenberg A. 1986. The occurrence of polyenoic fatty acids with greater than 22 carbon atoms in mammalian spermatozoa. *Biochem J.* 240(3):891–895.

Rabionet M, Van Der Spoel AC, Chuang CC, von Tumpling-Radosta B, Litjens M, Bouwmeester D, Hellbusch CC, Korner C, Wiegandt H, Gorgas K, et al. 2008. Male germ cells require polyenoic sphingolipids with complex glycosylation for completion of meiosis: A link to ceramide synthase-3. *J Biol Chem.* 283(19):13357–13369.

Robinson BS, Johnson DW, Poulos A. 1992. Novel molecular species of sphingomyelin containing 2-hydroxylated polyenoic very-long-chain fatty acids in mammalian testes and spermatozoa. *J Biol Chem.* 267(3):1746–1751.

Rodemer C, Thai TP, Brugger B, Kaercher T, Werner H, Nave KA, Wieland F, Gorgas K, Just WW. 2003. Inactivation of ether lipid biosynthesis causes male infertility, defects in eye development and optic nerve hypoplasia in mice. *Hum Mol Genet.* 12(15):1881–1895.

Shimma S, Sugiura Y, Hayasaka T, Hoshikawa Y, Noda T, Setou M. 2007. MALDI-based imaging mass spectrometry revealed abnormal distribution of phospholipids in colon cancer liver metastasis. *J Chromatogr B Anal Technol Biomed Life Sci.* 855(1):98–103.

Shimma S, Sugiura Y, Hayasaka T, Zaima N, Matsumoto M, Setou M. 2008. Mass imaging and identification of biomolecules with MALDI-QIT-TOF-based system. *Anal Chem.* 80(3):878–885.

Simons K, Ikonen E. 1997. Functional rafts in cell membranes. *Nature.* 387(6633):569–572.

Sugiura Y, Shimma S, Konishi Y, Yamada MK, Setou M. 2008. Imaging mass spectrometry technology and application on ganglioside study; Visualization of age-dependent accumulation of C20-ganglioside molecular species in the mouse hippocampus. *PLoS ONE.* 3(9):3232.

Tadano-Aritomi K, Ishizuka I. 2003. Structure and function of sulfoglycolipids in the kidney and testis. *Trends Glycosci Glycotech.* 15(81):15–27.

Tadano-Aritomi K, Matsuda J, Fujimoto H, Suzuki K, Ishizuka I. 2003. Seminolipid and its precursor/degradative product, galactosylalkylacylglycerol, in the testis of saposin A- and prosaposin-deficient mice. *J Lipid Res.* 44(9):1737–1743.

Ueno K, Ishizuka I, Yamakawa T. 1977. Glycolipid composition of human testis at different ages and the stereochemical configuration of seminolipid. *Biochim Biophys Acta.* 487(1):61–73.

Weerachatyanukul W, Rattanachaiyanont M, Carmona E, Furimsky A, Mai A, Shoushtarian A, Sirichotiyakul S, Ballakier H, Leader A, Tanphaichitr N.

2001. Sulfogalactosylglycerolipid is involved in human gamete interaction. *Mol Reprod Dev.* 60(4):569–578.

White D, Weerachatyanukul W, Gadella B, Kamolvarin N, Attar M, Tanphaichitr N. 2000. Role of sperm sulfogalactosylglycerolipid in mouse sperm-zona pellucida binding. *Biol Reprod.* 63(1):147–155.

Wierzbicki AS. 2007. Peroxisomal disorders affecting phytanic acid alpha-oxidation: A review. *Biochem Soc Trans.* 35(Pt 5):881–886.

Yao I, Sugiura Y, Matsumoto M, Setou M. 2008. In situ proteomics with imaging mass spectrometry and principal component analysis in the Scrapper-knockout mouse brain. *Proteomics.* 8(18):3692–3701.

Zhang Y, Hayashi Y, Cheng X, Watanabe T, Wang X, Taniguchi N, Honke K. 2005. Testis-specific sulfoglycolipid, seminolipid, is essential for germ cell function in spermatogenesis. *Glycobiology.* 15(6):649–654.